

## THE EFFECT OF TUNED-MASS DAMPERS ON THE SEISMIC RESPONSE OF BASE-ISOLATED STRUCTURES

HSIANG-CHUAN TSAI

Department of Construction Engineering, National Taiwan Institute of Technology, P.O. Box 90-130, Taipei, Taiwan, Republic of China

(Received 30 December 1993; in revised form 26 June 1994)

**Abstract**—The low stiffness of laminated rubber bearings utilized in base isolation could potentially cause large lateral displacements which must be reduced by some energy-dissipation mechanism. The effect of applying tuned-mass dampers towards reducing the lateral deformation of the isolators was studied in this paper. The choice of the proper parameters of the tuned-mass damper and the influence of excitation frequency on the response were investigated. Through the numerical simulation of a five-storey base-isolated building subjected to different earthquake records, it was found that although the tuned-mass damper had little effect on structural response during the first few seconds of earthquake excitation, the damper may add damping to the structure to reduce the subsequent response. The idea of the accelerated tuned-mass damper was proposed and demonstrated the capability of decreasing the maximum deformation of the isolators which occurred at the beginning of earthquake excitation.

### 1. INTRODUCTION

Base isolation is a new design philosophy for earthquake protection of structures in which a building is decoupled from the ground so that any damaging earthquake motion cannot be transmitted into the building. The most commonly used isolation system utilizes laminated rubber bearings (Kelly, 1987). Laminated rubber bearings can significantly reduce the acceleration response of a building; however, their low stiffness in the horizontal directions may potentially cause unacceptably large lateral displacements which must be reduced by some energy-dissipation mechanism, for example, high damping rubber bearings (Derham and Kelly, 1985), lead-filled rubber bearings (Robinson, 1982) or oil dampers (Kuroda *et al.*, 1989).

An aseismic hybrid control system was proposed by Yang *et al.* (1991) which combines rubber bearings and a passive tuned-mass damper. Numerical analysis was carried out on a 20-storey building subjected to a simulated earthquake ground acceleration and the proposed system was observed to be capable of effectively lowering the structural response. This observation would imply that the tuned-mass damper could be employed as an energy-dissipation device towards minimizing the deformation of rubber bearings.

Passive tuned-mass dampers have been successfully applied in high-rise buildings toward reducing the vibration induced by the wind (Petersen, 1980). However, general agreement has not been reached about the adequacy of tuned-mass dampers in reducing the response of structures to earthquake vibrations (Kaynia *et al.*, 1981). Several reasons arise why the results from numerous studies on the seismic-response reduction are quite contradictory. First of all, the earthquake motion may possibly induce multiple-mode responses for tall buildings. A single damper tuned to the fundamental mode of a building may not be effective in significantly reducing earthquake-induced motion (Clark, 1988). Secondly, the damper parameters used in these studies may not be the optimum values for the systems excited by ground motion (Villaverde, 1985). Thirdly, a tuned-mass damper which is a passive device requires the motion of the primary structure to react with. For an earthquake excitation in which its duration is substantially shorter than wind excitation, the tuned-mass damper may not have time to produce a significant effect (Sladek and Klingner, 1983).

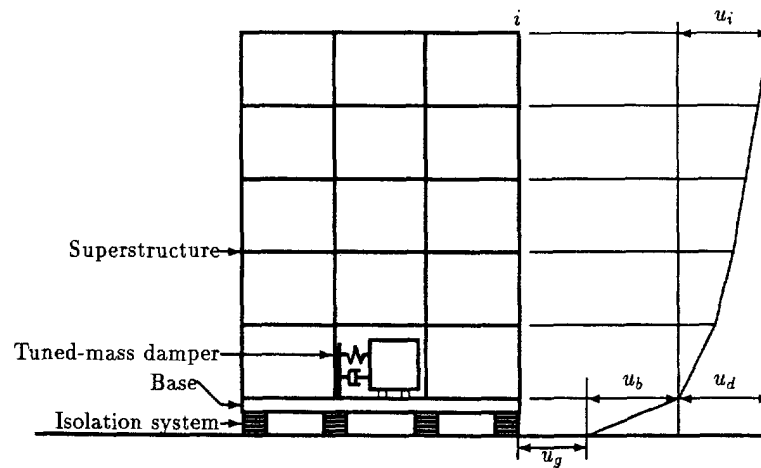


Fig. 1. Base-isolated structure with tuned-mass damper.

Similar results may arise whenever applying the tuned-mass damper towards base isolation as an energy-dissipation device. More intensive research on the factors which affect the performance of tuned-mass dampers towards reducing the seismic response of base-isolated structures becomes necessary, since only one simulated earthquake acceleration was chosen as the input in the study of Yang *et al.* (1991). The choice of the proper parameters of the tuned-mass damper and the influence of excitation frequency on the response are investigated in this paper. The responses of a five-storey base-isolated structure with a tuned-mass damper are analyzed by using various real earthquake records. The effect of the tuned-mass damper on reducing the deformation of the isolator is then discussed. A semi-active tuned-mass damper, referred to as the accelerated tuned-mass damper, which can effectively reduce the maximum displacement of the isolator is finally proposed.

The combined structure-damper systems possess three dynamic characteristics which must be considered in the present analysis. The first is tuning, which causes the damper vibration in resonance. The second is interaction, which is the feedback effect between the motions of the damper and the structure. The third is non-classical damping, which occurs as a result of the various damping characteristics among the damper, the structure and the isolator. The light equipment in base-isolated structures has similar dynamic characteristics, the seismic response of which can be accurately solved, not by using the classic mode method, but by using the complex mode method (Tsai and Kelly, 1988). An efficient algorithm for the complex mode method is introduced in this paper and applied towards calculating the seismic response of base-isolated structures with tuned-mass dampers.

## 2. SOLUTION SCHEME

The two-dimensional model of a base-isolated building equipped with a tuned-mass damper is shown in Fig. 1 where only horizontal degrees of freedom are considered. The base of the isolated structure is treated as a rigid lumped mass,  $m_b$ , and its displacement relative to the ground is denoted as  $u_b$ . The isolation system has lateral stiffness  $k_b$ , and damping  $c_b$ . The tuned-mass damper is modeled as a mass  $m_d$ , stiffness  $k_d$  and damping  $c_d$ . The displacement of the tuned-mass damper relative to the base is denoted as  $u_d$ . The superstructure has  $n$  degrees of freedom. The  $i$ th superstructural degree of freedom has a lumped mass  $m_i$ . The corresponding displacement components  $u_i$  represent the superstructural deformation relative to the base. The total structural mass is  $m_f = m_b + \sum_{i=1}^n m_i$ . The response of this base isolation model excited by a ground acceleration  $\ddot{u}_g$  is governed by the following equations

$$(m_f + m_d)\ddot{u}_b + m_d\ddot{u}_d + \sum_{i=1}^n m_i\ddot{u}_i + c_b\dot{u}_b + k_b u_b = -(m_f + m_d)\ddot{u}_g \quad (1)$$

$$m_d\ddot{u}_b + m_d\ddot{u}_d + c_d\dot{u}_d + k_d u_d = -m_d\ddot{u}_g \quad (2)$$

$$m_i\ddot{u}_b + m_i\ddot{u}_i + \sum_{j=1}^n c_{ij}\dot{u}_j + \sum_{j=1}^n k_{ij}u_j = -m_i\ddot{u}_g \quad (3)$$

for  $i = 1, \dots, n$ , in which  $c_{ij}$  and  $k_{ij}$  are the entries of the damping and stiffness matrices of the superstructure.

The above three equations can be combined to obtain

$$\mathbf{M}\ddot{\mathbf{u}} + \mathbf{C}\dot{\mathbf{u}} + \mathbf{K}\mathbf{u} = -\mathbf{M}\mathbf{r}\ddot{u}_g \quad (4)$$

where

$$\mathbf{u} = [u_b \quad u_d \quad u_1 \quad \dots \quad u_n]^T \quad (5)$$

and

$$\mathbf{r} = [1 \quad 0 \quad 0 \quad \dots \quad 0]^T. \quad (6)$$

This is the equation of motion for a system of  $n+2$  degrees of freedom. Equation (4) could be solved by the classic mode method, if the matrix  $\mathbf{C}$  were approximated to be in proportion to the mass and stiffness matrices. However, this approximation can cause a large error if the system contains the tuned light mass (Tsai and Kelly, 1988). To be exactly solved, eqn (4) must be reformulated into a first-order  $2(n+2)$ -dimensional system of equations (Hurty and Rubinstein, 1964),

$$\mathbf{A}\dot{\mathbf{v}} + \mathbf{B}\mathbf{v} = -\mathbf{F}\ddot{u}_g \quad (7)$$

in which

$$\mathbf{A} = \begin{bmatrix} \mathbf{0} & \mathbf{M} \\ \mathbf{M} & \mathbf{C} \end{bmatrix}; \quad \mathbf{B} = \begin{bmatrix} -\mathbf{M} & \mathbf{0} \\ \mathbf{0} & \mathbf{K} \end{bmatrix}; \quad \mathbf{F} = \begin{Bmatrix} \mathbf{0} \\ \mathbf{M}\mathbf{r} \end{Bmatrix}; \quad \mathbf{v} = \begin{Bmatrix} \dot{\mathbf{u}} \\ \mathbf{u} \end{Bmatrix}. \quad (8)$$

The associated eigenproblem equation is of order  $2(n+2)$  which can be expressed as

$$\mathbf{B}\Psi_i = -p_i\mathbf{A}\Psi_i \quad (9)$$

where  $p_i$  and  $\Psi_i$  are the  $i$ th eigenvalue and eigenvector. Since matrices  $\mathbf{A}$  and  $\mathbf{B}$  are symmetrical but are not positive definite,  $p_i$  and  $\Psi_i$  will be complex in value and occur in conjugate pairs. The eigenvectors  $\Psi_i$  can be simplified according to the definition of  $\mathbf{v}$  in eqn (8) as

$$\Psi_i = \begin{Bmatrix} p_i\Phi_i \\ \Phi_i \end{Bmatrix} \quad (10)$$

where  $\Phi_i$  is the eigenvector corresponding to the displacement components.

Applying the orthogonal property of eigenvectors and the transformation

$$\mathbf{v} = \sum_{i=1}^{2(n+2)} \mathbf{Z}_i \Psi_i \quad (11)$$

where  $\mathbf{Z}_i$  are the generalized coordinates to be solved, eqn (7) can be decoupled to  $2(n+2)$  independent differential equations

$$\dot{Z}_i - p_i Z_i = -N_i \ddot{u}_g \quad (12)$$

in which  $N_i$  is the participation factor defined as

$$N_i = \frac{\Psi_i^T \mathbf{F}}{\Psi_i^T \mathbf{A} \Psi_i} = \frac{\Phi_i^T \mathbf{M} \mathbf{r}}{2p_i \Phi_i^T \mathbf{M} \Phi_i + \Phi_i^T \mathbf{C} \Phi_i} \quad (13)$$

The solution of  $Z_i$  is  $N_i h_i(t)$  with

$$h_i(t) = e^{p_i t} h_i(0) - \int_0^t e^{p_i(t-\tau)} \ddot{u}_g(\tau) d\tau \quad (14)$$

where  $h_i(0)$  is derived from the initial condition of  $\mathbf{v}$ ,

$$h_i(0) = \frac{\Psi_i^T \mathbf{A} \mathbf{v}(0)}{\Psi_i^T \mathbf{F}} \quad (15)$$

The values of  $h_i(t)$  for varied  $t$  could be computed by any numerical integration method. However, if the ground acceleration is piecewise linear and defined at time series  $t_k$ , the integration in eqn (14) can be explicitly derived and  $h_i(t)$  can be calculated by the following algorithm

$$\dot{h}_i(t_k) = \left( \dot{h}_i(t_{k-1}) - \frac{s_{k-1}}{p_i} \right) e^{p_i(t_k - t_{k-1})} + \frac{s_{k-1}}{p_i} \quad (16)$$

$$h_i(t_k) = \frac{\dot{h}_i(t_k) + f_k}{p_i} \quad (17)$$

where  $f_k$  is the ground acceleration  $\ddot{u}_g$  at time  $t_k$  and  $s_k = (f_k - f_{k-1}) / (t_k - t_{k-1})$ . If the ground acceleration is defined at constant time interval, the exponential term in eqn (16) is constant for different  $t_k$  and can be calculated before the algorithm is proceeded with. The algorithm becomes very efficient in the light of only three multiplication operations of complex number being required for each time step.

Following eqn (11), the displacement vector can be found by the combination of all modes

$$\mathbf{u} = \sum_{i=1}^{2(n+2)} N_i h_i(t) \Phi_i \quad (18)$$

Only  $n+2$  modes are, in practical application, required in the combination, since  $N_i$ ,  $h_i$  and  $\Phi_i$  are complex and occur in conjugate pairs.

### 3. PARAMETERS OF TUNED-MASS DAMPERS

Choosing the proper parameters of tuned-mass dampers is an important factor which affects the performance of tuned-mass dampers towards reducing the seismic response. When studying the parameters of tuned-mass dampers, the primary structure of concern is

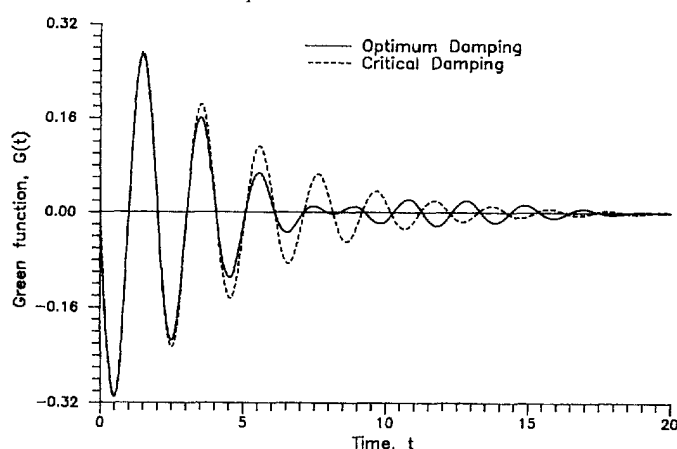


Fig. 2. Green's functions of optimum damping and critical damping ( $\xi_p = 0.02$ ,  $\gamma = 0.04$  and  $f = 0.943$ ).

generally simplified as a main mass of which the natural frequency is denoted as  $\omega_p$  and the damping ratio is  $\xi_p$ . The mass of tuned-mass dampers is expressed by the mass ratio,  $\gamma$ , that is, the ratio of the damper mass to the main mass. The stiffness of tuned-mass dampers is represented by the tuning frequency ratio,  $f$ , that is, the ratio of the natural frequency of the damper to that of the primary structure. The damping ratio of the tuned-mass damper is denoted by  $\xi_s$ .

The optimum tuning frequency and damping ratio of the tuned-mass damper which can minimize the steady-state response of the damped primary structures have been derived (Tsai and Lin, 1993) as

$$f = \left( \frac{\sqrt{1-0.5\gamma}}{1+\gamma} + \sqrt{1-2\xi_p^2} - 1 \right) - (2.375 - 1.034\sqrt{\gamma} - 0.426\gamma)\sqrt{\gamma}\xi_p - (3.730 - 16.903\sqrt{\gamma} + 20.496\gamma)\sqrt{\gamma}\xi_p^2 \quad (19)$$

$$\xi_s = \sqrt{\frac{3\gamma}{8(1+\gamma)(1-0.5\gamma)}} + (0.151\xi_p - 0.170\xi_p^2) + (0.163\xi_p + 4.980\xi_p^2)\gamma. \quad (20)$$

For the transient response, it has been found (Tsai, 1993) that there exists a critical damping level for tuned-mass dampers which is equal to  $\xi_p + \sqrt{\gamma}$ . Increasing damping in the damper would enhance the Green's function of structural response whenever the damper damping  $\xi_s$  is larger than the critical value. When the damper damping is smaller than the critical value, the Green's function develops beat phenomena. The structure with a damper of less damping would have a smaller response in the first beat cycle, but also have a higher rebound in the following cycles.

The optimum damping defined in eqn (20) is observed to be smaller than the critical damping of the Green's function. For the case of  $\gamma = 0.04$  and  $\xi_p = 0.02$ , the critical damping is 0.22 and the optimum parameters calculated from eqns (19) and (20) are  $f = 0.943$  and  $\xi_s = 0.125$ . Having the same tuning frequency, the Green's functions of structural response using the critical damping and the optimum damping are plotted in Fig. 2, which indicates that the optimum damping has a smaller response than the critical damping and a high rebound would not occur. This phenomena suggests that the optimum parameters obtained from the steady-state response can be applied for the transient response.

To investigate whether the optimum parameters obtained from eqns (19) and (20) are suitable or not for the real earthquake response, the responses of a primary mass excited by the El Centro record are computed for various damper dampings and compared in Fig.

3. The solution scheme described in the last section is applied except that the superstructural degrees of freedom are neglected. In Fig. 3(a), around the 10th s of the response histories, the lower  $\xi_s$  is shown to have a smaller response; however, the beating effect occurs around the 15th s. Figure 3(b) shows that damping which is larger than the critical value has a higher response. Figure 3(c) reveals that the response of the optimum damping is lower than that of the critical value and beat rebound is not high. Consequently, the optimum parameters obtained from the steady-state response can be adopted as the proper parameters for the seismic response.

Villaverde (1985) has recommended using the critical damping ratio,  $\xi_p + \sqrt{\gamma}$ , as the damping ratio of the tuned-mass dampers, on the basis of the phenomenon that response spectrum ordinates always decrease as the damping increases. However, this situation is shown in Figs 2 and 3 to be untrue. Response spectrum method is based on the classical mode theory which, as mentioned before, may potentially create a large error when applied towards solving the tuned-mass damper problem.

#### 4. INFLUENCE OF INPUT FREQUENCY

Another factor which can affect the performance of tuned-mass dampers is the characteristics of input accelerations. The variations of steady-state responses with input frequencies are plotted in Fig. 4 for different sizes of optimum dampers. This figure demonstrates that increasing the mass ratio,  $\gamma$ , can reduce peak amplitudes; however, for input frequencies that are lower than the frequency of the first peak, increasing the mass ratio will enhance response amplitudes because of wider separation between the two peaks. For high input frequencies, the damper has little effect on reducing the structural response.

Similar results can be observed from the transient responses of the primary structure excited by the harmonic ground motions with three different input frequencies shown in Fig. 5. The acceleration of ground motions is defined as

$$\ddot{u}_g(t) = \begin{cases} 0.25H \sin(\omega t) & \text{for } 0 \leq t \leq \pi/\omega \\ 0.75H \sin(\omega t) & \text{for } \pi/\omega \leq t \leq 2\pi/\omega \\ H \sin(\omega t) & \text{for } 2\pi/\omega \leq t \end{cases} \quad (21)$$

where  $\omega$  is the input frequency and  $H$  is the input amplitude which is set to be  $1 \text{ m/s}^2$ . The corresponding displacement function oscillates about the zero base line simulating real earthquake records. The structural parameters used are  $\omega_p = 0.503 \text{ Hz}$ ,  $\xi_p = 0.05$ ,  $\gamma = 0.05$ ,  $f = 0.914$  and  $\xi_s = 0.143$ , which are obtained from eqns (19) and (20).

The displacement responses of the primary structure excited by impulsive ground motions with different durations are shown in Fig. 6. The input acceleration is defined as

$$\ddot{u}_g(t) = \begin{cases} H \sin(4\pi t/T) & \text{for } 0 \leq t \leq T/4 \\ H \cos(2\pi t/T) & \text{for } T/4 \leq t \leq 3T/4 \\ -H \sin(4\pi t/T) & \text{for } 3T/4 \leq t \leq T \\ 0 & \text{for } T \leq t \end{cases} \quad (22)$$

The corresponding displacement function is an impulse of duration  $T$ . After the impulse excitation, the response of the structure having the tuned-mass damper decays faster than that without the damper. However, the damper does not have any effect during the first cycle of the responses and the structural response is the same as that without the damper. For an impulse excitation of long duration, that is, 4.0 s, the first few peaks of the response of the structure with the damper are higher than that without the damper. This occurs as a result of the excitation frequency being lower than the natural frequency of the structure, that is, the same reverse effect indicated in Fig. 4.

The natural frequency of the base isolation system is generally below the dominant frequency range of earthquakes. The frequency contents of earthquakes which would

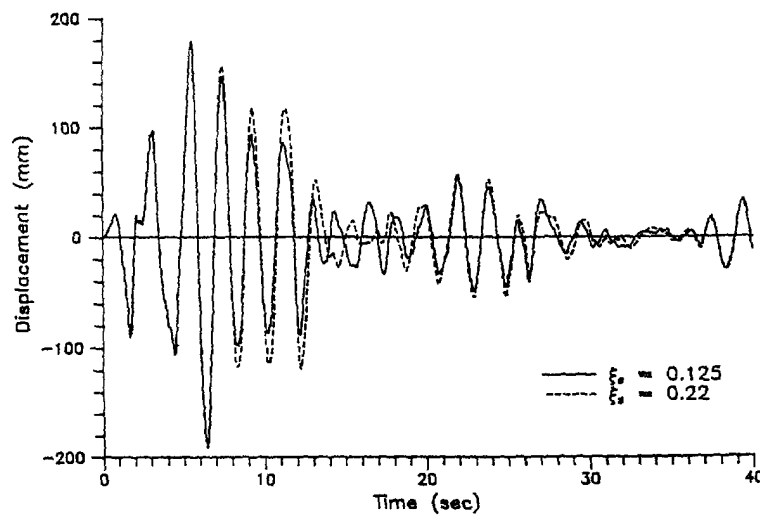
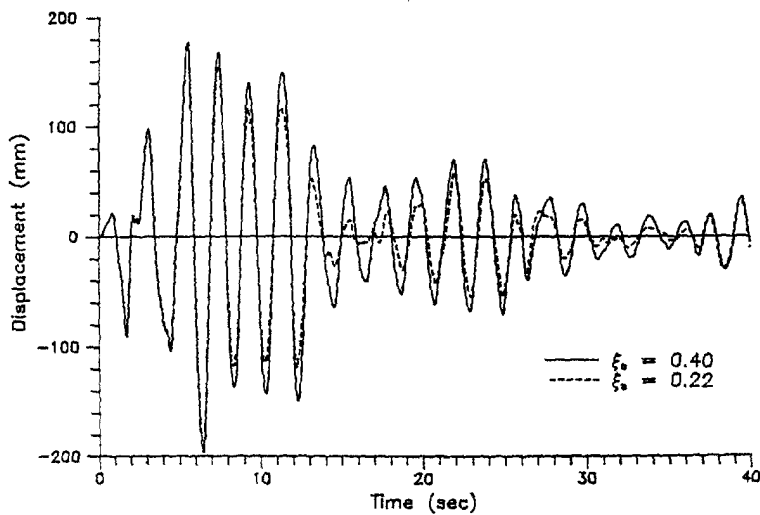
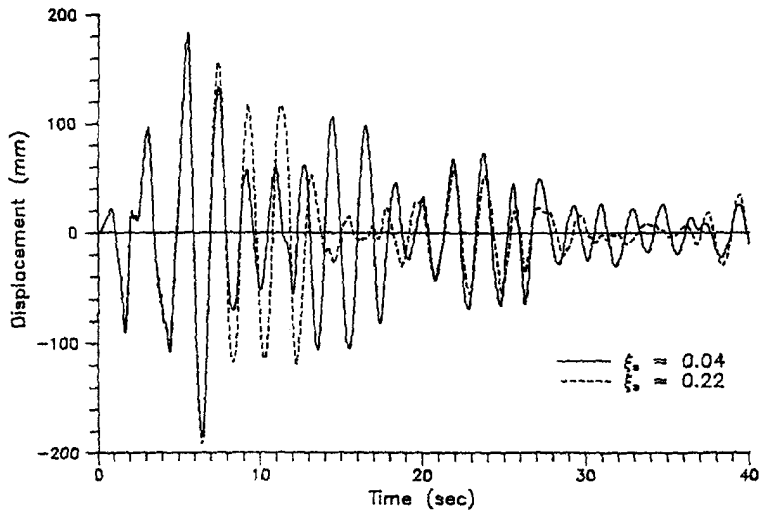


Fig. 3. Displacement response for damper damping (a) smaller than critical value, (b) larger than critical value and (c) equal to optimum value ( $\omega_p = 0.5$  Hz,  $\xi_p = 0.02$ ,  $\gamma = 0.04$  and  $f = 0.943$ ).

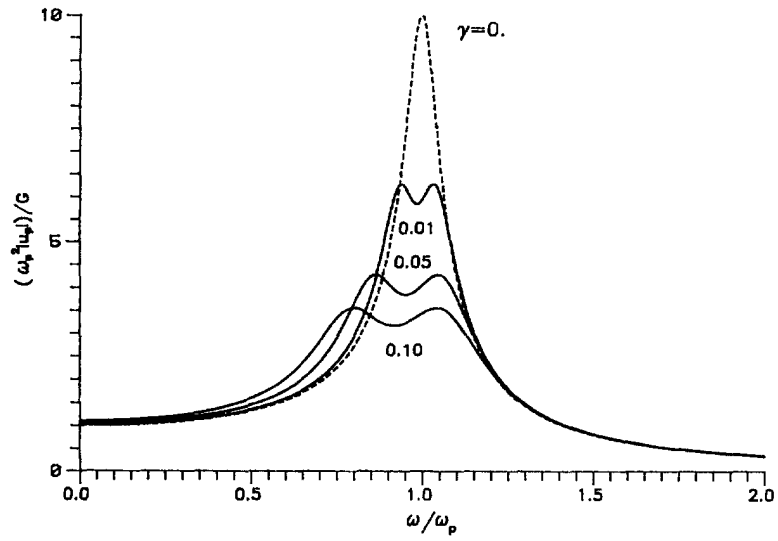


Fig. 4. Steady-state response of primary structure ( $\zeta_p = 0.05$ ) with optimum tuned-mass damper.

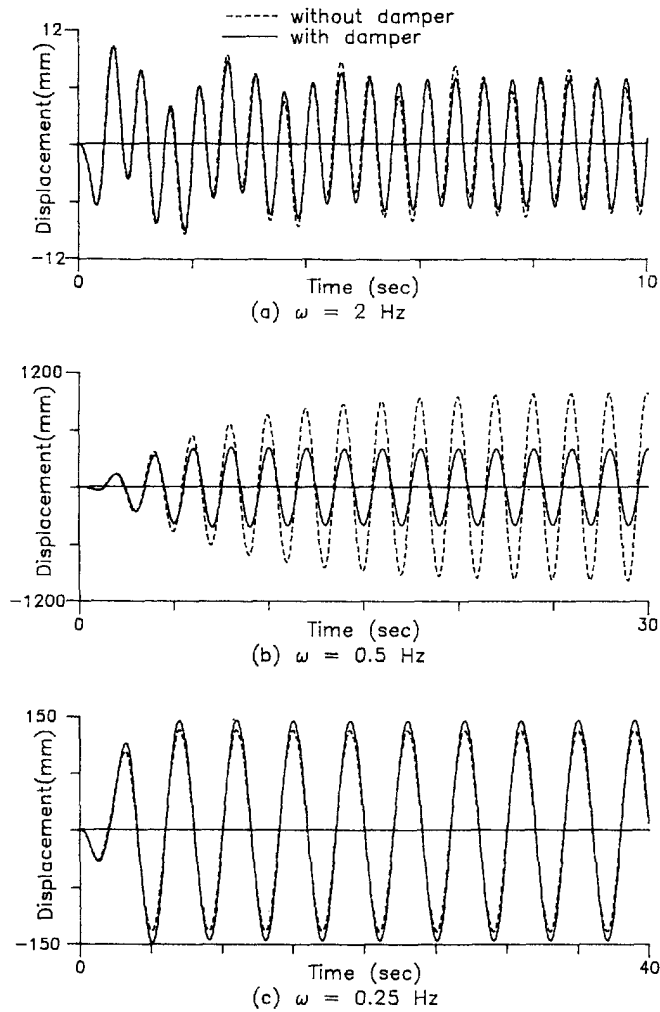


Fig. 5. Displacement responses excited by harmonic ground motion with frequency (a) higher than, (b) near to, (c) lower than the natural frequency of structure.



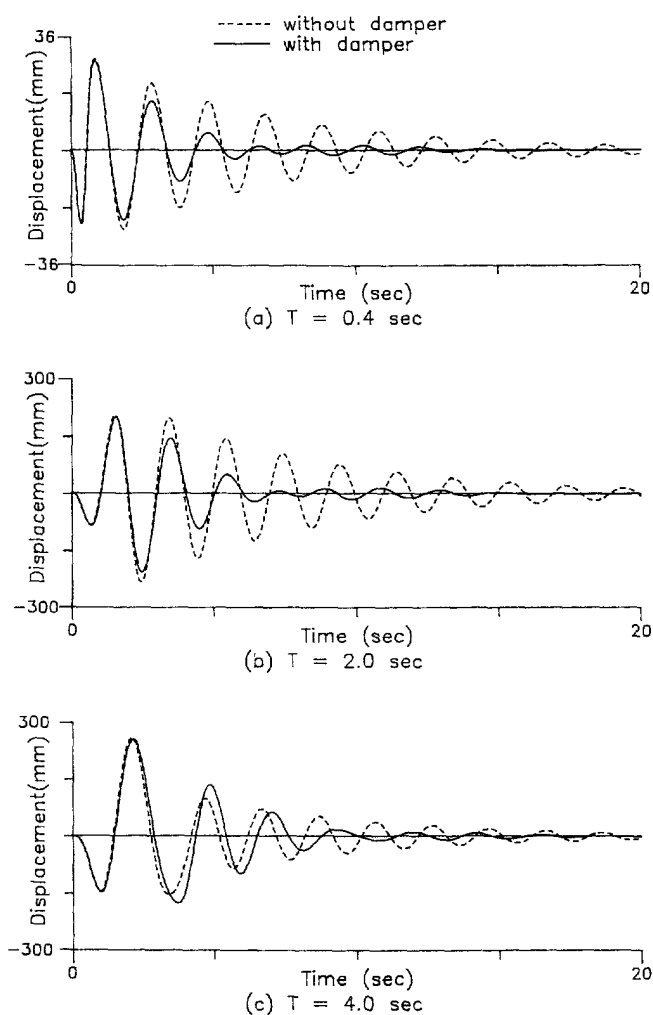


Fig. 6. Displacement response excited by impulsive ground motion with duration (a) shorter than, (b) equal to, and (c) longer than the natural period of structure.

become amplified by the tuned-mass damper are very small in base isolation systems. This is a virtue of using the tuned-mass damper for base-isolated structures.

##### 5. RESPONSE OF BASE-ISOLATED STRUCTURES

In the light of a large variation in stiffness between the isolators and the superstructure, the superstructural deformation is always much smaller than the deformation of the isolators, especially at the fundamental vibration mode in which the deformation of superstructural components is negligible. Reducing the vibration of the first mode can significantly decrease the deformation of the isolators. Consequently, a single damper tuned to the fundamental mode is adequate for reducing the earthquake vibration of base-isolated buildings. This is yet another advantage of using the tuned-mass damper for base-isolated structures.

The base isolation model used in the numerical simulation is a five-storey building which can be simplified as a six-degree-of-freedom system. Each floor in the superstructure has the same mass, 3500 kg, the same stiffness, 35 kN/mm, and the same damping, 35 Ns/mm. If the superstructure is assumed to be fixed at the base, the natural frequency of the superstructure is 4.5 Hz and the corresponding damping ratio is 0.014. The mass of the base,  $m_b$ , is 3500 kg. The total mass of the base-isolated structure,  $m_r$ , is 21000 kg. The numerical simulation is carried out on two types of isolation systems which have the same

stiffness but different dampings. The stiffness of the isolation system,  $k_b$ , is 0.21 kN/mm and the natural frequency of the base isolation system,  $\omega_b = \sqrt{k_b/m_f}$ , is equal to 0.503 Hz. One type of isolation system has a lower damping level  $c_b = 2.66$  Ns/mm, which corresponds to the damping ratio,  $\xi_b = c_b/(2\omega_b m_f)$ , equal to 0.02. The other type has a higher damping level  $c_b = 6.64$  Ns/mm, which corresponds to  $\xi_b = 0.05$ . The mass of the damper,  $m_d$ , is 1050 kg, which corresponds to a mass ratio of  $\gamma = m_d/m_f = 0.05$ . The tuning frequencies and damping ratios were obtained from the optimum parameters of the steady-state response in eqns (19) and (20) by assuming that  $\omega_p = \omega_b$  and  $\zeta_p = \zeta_b$ .

The displacement histories at the base of the isolated structure excited by the four earthquake records are plotted in Fig. 7 for  $\xi_b = 0.02$  and Fig. 8 for  $\xi_b = 0.05$ , where the responses using the optimum damper are compared with the responses without the damper. The responses of the structures with the dampers are inferred from these figures to display a quick decay, except for the first few seconds in which the responses are close to those without the dampers. The tuned-mass damper is shown, from a comparison of Fig. 8 with Fig. 7 to be more effective on the isolation system with a lower damping level.

The reduction ratio, defined as the ratio of the maximum base displacement of the structure with the damper to that without damper, can be regarded as an index which demonstrates the effectiveness of the tuned-mass damper acting as an energy-dissipation device of the base isolation system. The variation of the reduction ratios with different damper masses are plotted in Fig. 9 for four earthquake records and two types of isolator damping, which shows that the values of the reduction ratios are quite influenced by the earthquake records. The tuned-mass damper can effectively reduce the maximum base displacements when the structure is excited by the Taft record and the Parkfield record. The values of the reduction ratios have a tendency to decrease as the dampers become heavier; however, the decrease curtails after the mass ratios become greater than some values. The heavier damper is indicated from eqn (20) to have a higher optimum damping and so have a faster decay in response, which causes the time when the maximum displacement peak occurs to move to the beginning of the history. However, since the damper has little effect on reducing the response at the beginning of the excitation, the maximum displacement becomes unchanged as the mass of the optimum damper continues to increase. For the Pacoima Dam record, the reduction by the tuned-mass damper becomes less effective in the light of the fact that the maximum responses happen very early, as shown in Figs. 7(d) and 8(d). The variation of the maximum displacements with the damper masses for the El Centro record is very peculiar. The maximum response is enhanced by the heavier damper, whenever the mass ratios are greater than some value. As shown in Figs 7(a) and 8(a), the structure with the damper notably has a higher response at the peaks near the 5th s than that without the damper. The reasonable explanation is that the El Centro record contains some low-frequency energy during the first few seconds. The peculiar phenomenon in which heavier dampers can create a higher maximum displacement could appear whenever the maximum displacement occurs on one of the peaks near the 5th s.

## 6. ACCELERATED TUNED-MASS DAMPERS

The tuned-mass damper, which is a passive device, requires the motion of the primary structure to react; consequently, the tuned-mass damper has little effect on the structural response in the first few seconds of the excitation. The tuned-mass damper exerts no effect towards reducing the maximum deformation of the isolator, if the maximum response occurs early in the earthquake record. Accelerating the motion of the tuned-mass damper at the beginning of the excitation is one way of making the tuned-mass damper react earlier in earthquake excitation.

Accelerating the tuned-mass damper requires careful examination because unsuitable acceleration may potentially enhance the deformation of the isolator. When the deformation of the isolator reaches one of the peaks, applying an impulse towards the damper in the same direction of the isolator displacement can accelerate the damper and also create a pull force to the isolator which can consequently reduce the deformation of the isolator at the next peak. A threshold value is set for the deformation of the isolator, since not every

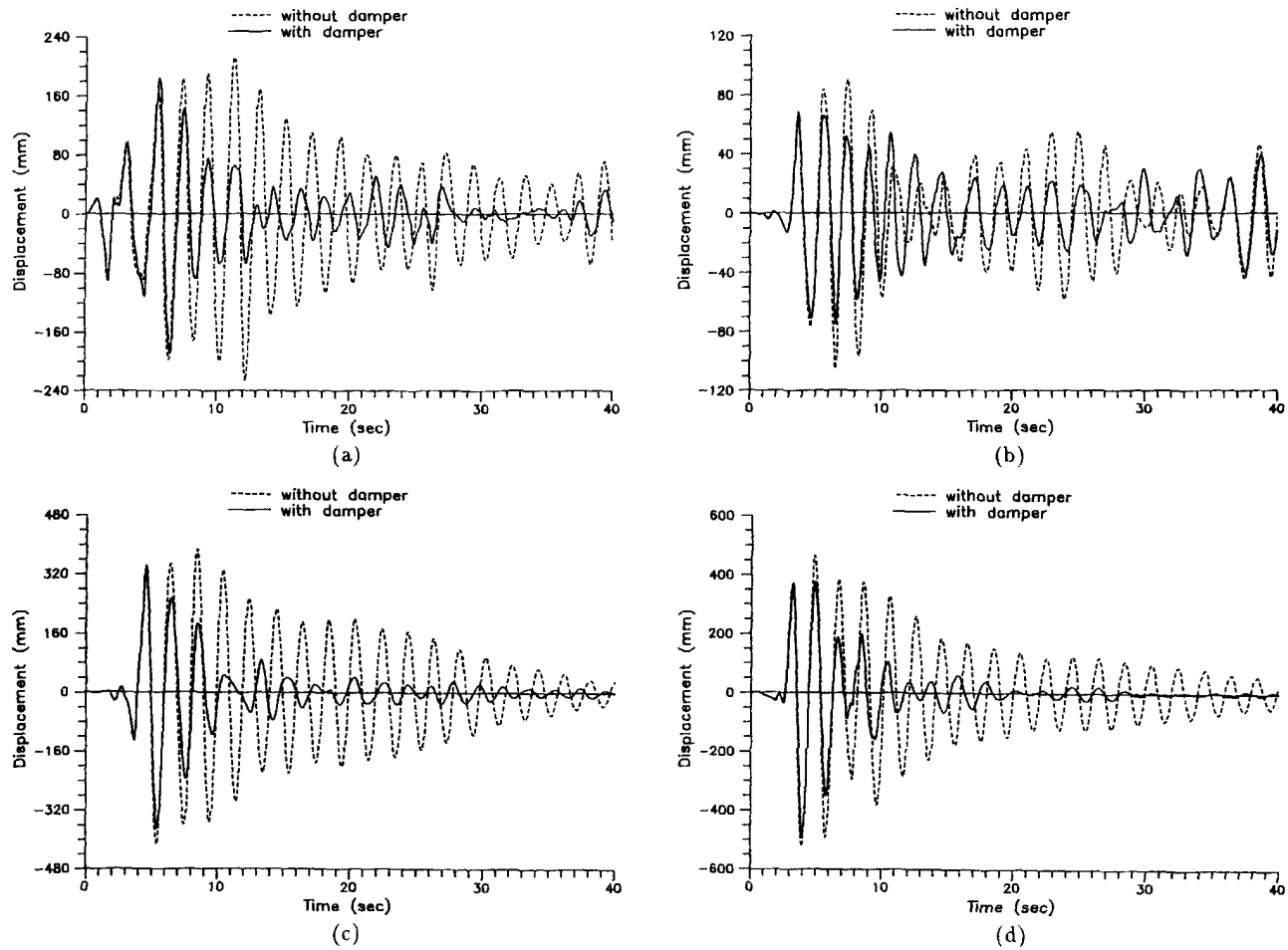


Fig. 7. Base displacement response excited by (a) El Centro record, (b) Taft record, (c) Parkfield record, (d) Pacoima Dam record, for  $\zeta_b = 0.02$ .

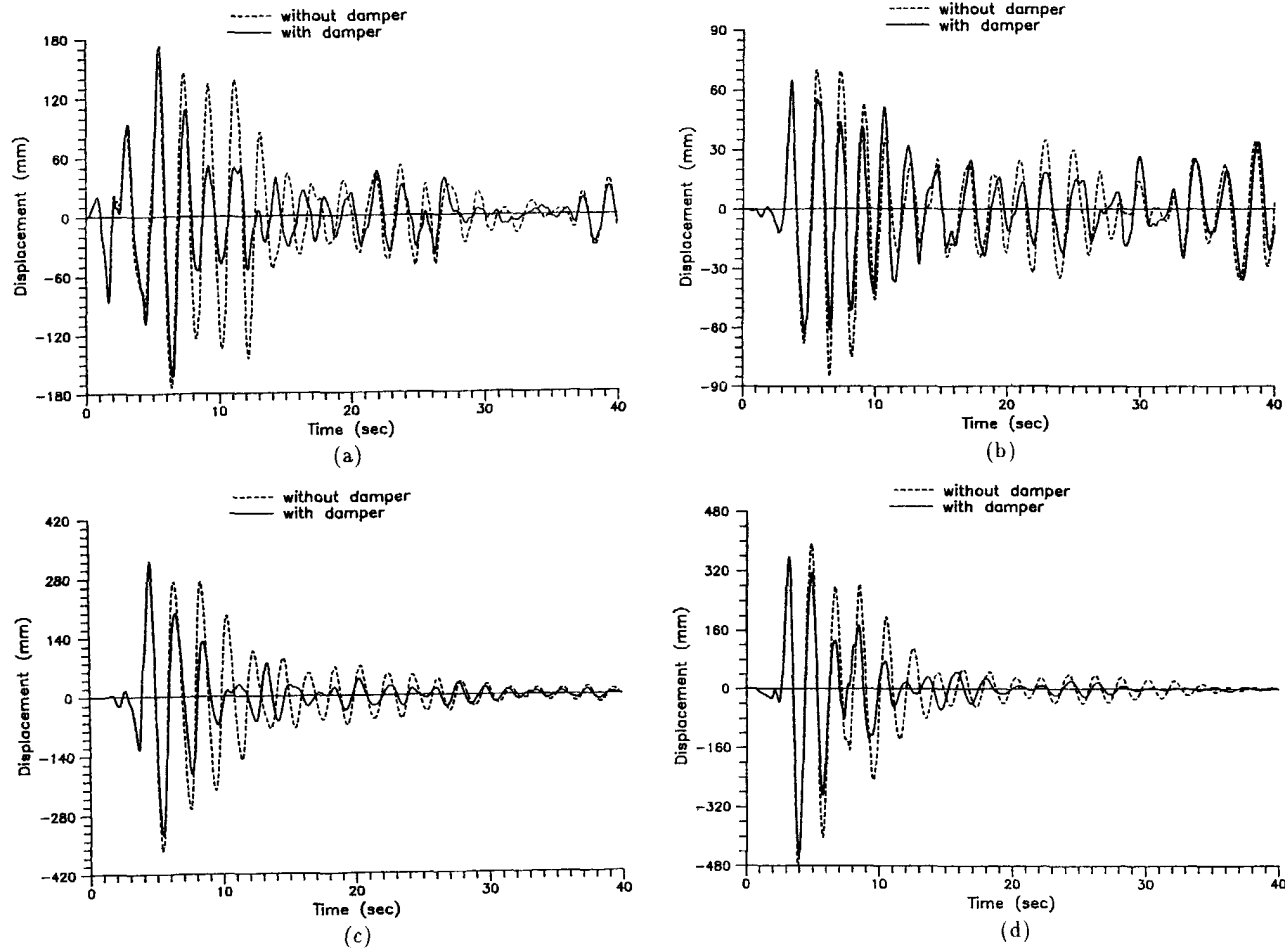


Fig. 8. Base displacement response excited by (a) El Centro record, (b) Taft record, (c) Parkfield record, (d) Pacoima Dam record, for  $\xi_b = 0.05$ .

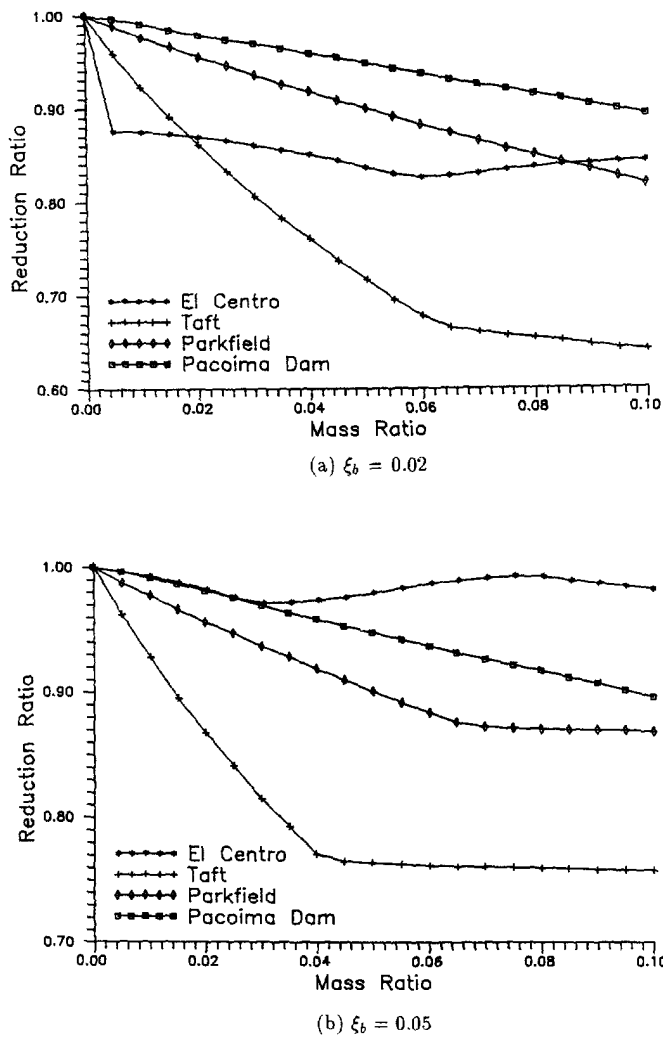


Fig. 9. Variation of maximum base displacement with damper mass for (a)  $\xi_b = 0.02$  and (b)  $\xi_b = 0.05$ .

earthquake excitation is so severe that the tuned-mass damper must be accelerated every time. The deformation of the isolator is monitored during the earthquake excitation. The velocity of the tuned-mass damper is increased to a fixed value, whenever the deformation peak of the isolator is over the threshold value.

The feasibility of the accelerated tuned-mass damper is confirmed by modelling the base-isolated structure as a main mass having the natural frequency of  $\omega_p = 0.5$  Hz and a damping ratio of  $\xi_p = 0.02$ . The mass ratio of the damper is  $\gamma = 0.04$  and the optimum parameters of  $f = 0.943$  and  $\xi_s = 0.125$  are used. The velocity of the tuned-mass damper is accelerated to be 5 m/s when the deformation of the isolator reaches the first peak, which is more than 100 mm.

The displacement responses of the main mass equipped with the accelerated tuned-mass damper are plotted in Fig. 10 for the excitation of the four different earthquakes. The intensity of the Taft record has been magnified four times so that the deformation of the isolator can reach over the threshold value of 100 mm. The response curves of the passive tuned-mass damper without accelerator are also shown in this figure, which reveals that the accelerator causes the decay of the response to occur earlier. As far as the maximum displacement is concerned, the accelerated tuned-mass damper has a 24% reduction for the Parkfield record and 12% reduction for the Taft record and the Pacoima Dam record. For the El Centro record, the tuned-mass damper accelerated at the peak of the 3rd s has little

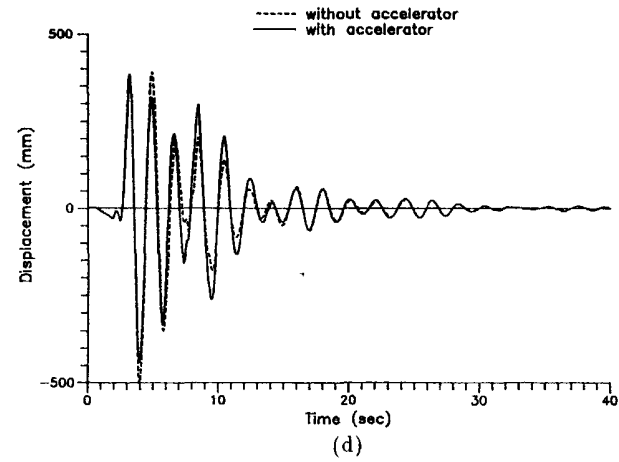
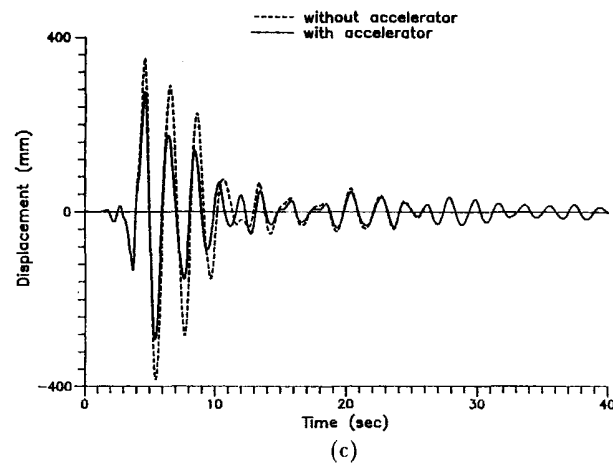
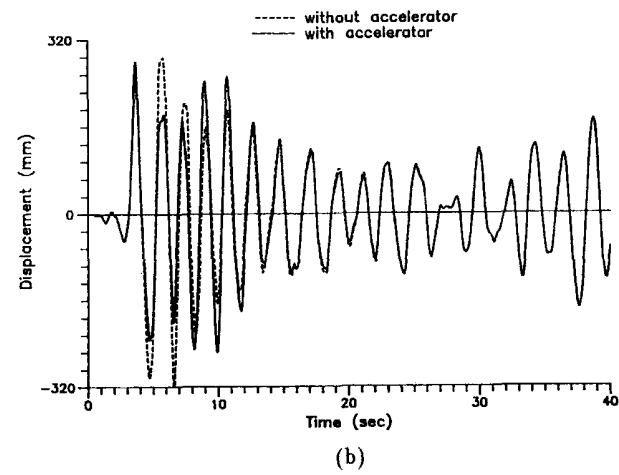
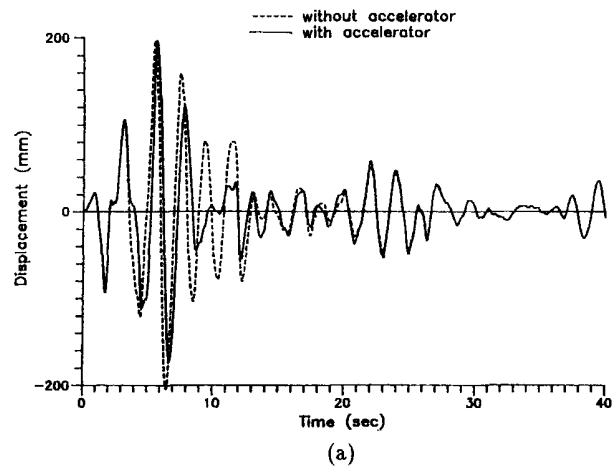


Fig. 10. Response excited by (a) El Centro record, (b) Taft record, (c) Parkfield record, (d) Pacoima Dam record, using accelerated tuned-mass damper.

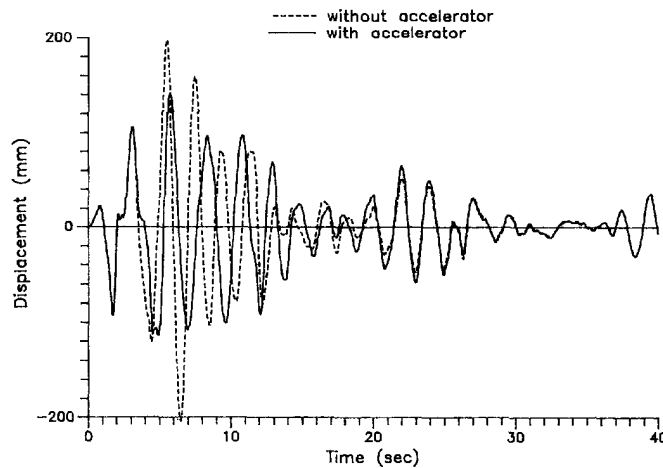


Fig. 11. Responses excited by El Centro record, using twice-accelerated tuned-mass damper.

effect on the maximum displacement at the 5th s; however, it can reduce the subsequent deformation.

Figure 10(a) suggests that accelerating the tuned-mass damper once is possibly not enough to reduce the maximum displacement. If the damper is accelerated twice, the maximum displacement is shown in Fig. 11 to have a 30% reduction for the El Centro record. Accelerating twice has little effect for the other three records because the second acceleration is functioning on or after the maximum peak.

## 7. CONCLUSION

The factors which affect the performance of the tuned-mass dampers on the seismic response of base-isolated structures were investigated from three aspects, that is, the tuned-mass dampers, the input earthquakes and the base-isolated structures.

There exists a critical value for the damper damping. If the damper damping is higher than this value, the tuned-mass damper would not reduce but rather enhance the structural response. The optimum tuning frequency and damping ratio of the tuned-mass damper obtained from the steady-state response provides a good guideline for the design of the tuned-mass damper to be applied towards reducing the seismic response of base-isolated structures.

The response on base-isolated structures equipped with the tuned-mass damper is quite dependent on the input earthquake motions. Adding the tuned-mass damper to the structure would enhance the structural response if the input frequency is lower than the natural frequency of the structure. This is not serious for base isolation because the natural frequency of base-isolated structures is generally lower than the dominant frequency of real earthquakes.

A single damper tuned to the fundamental mode is adequate for reducing the seismic response of base-isolated buildings, because the fundamental mode of base-isolated structures is nearly a rigid body mode which dominates in earthquake vibrations. Although the passive tuned-mass damper has little effect on the structural response during the first few seconds of earthquake excitation, the damper can add damping to the structure to reduce the subsequent response, as indicated from the numerical simulation on the base-isolated buildings subjected to the excitation of four earthquake records. The reduction by the tuned-mass damper becomes more prominent if the isolation system has less damping.

If the maximum response occurs early in the earthquake excitation, using the accelerated tuned-mass damper can effectively decrease the maximum deformation of the isolator. However, the proposal for the accelerated tuned-mass damper presented in this paper is only conceptual and idealistic. The issues of practicality and reliability of the accelerated tuned-mass damper remain to be resolved.

*Acknowledgment*—The research work reported in this paper was supported by the National Science Council, Republic of China, under grant No. NSC 80-0410-E011-02. This support is greatly appreciated.

## REFERENCES

- Clark, A. J. (1988). Multiple passive tuned mass dampers for reducing earthquake induced building motion. In *Proc. 9th World Conf. on Earthquake Engng.*, Tokyo, Japan, Vol. 5, pp. 779–784.
- Derham, C. J. and Kelly, J. M. (1985). Combined earthquake protection and vibration isolation. *Natural Rubber Technol.* **16**, 3–11.
- Hurty, W. C. and Rubinstein, M. F. (1964). *Dynamics of Structures*. Prentice-Hall, Englewood Cliffs, NJ.
- Kaynia, A. M., Veneziano, D. and Biggs, J. M. (1981). Seismic effectiveness of tuned mass dampers. *J. Struct. Div. ASCE* **107**(8), 1465–1484.
- Kelly, J. M. (1987). Recent developments in seismic isolation. 1987 *ASME Pressure Vessels and Piping Conference*, San Diego, California, PVP-127, pp. 381–385.
- Kuroda, T., Saruta, M. and Nitta, Y. (1989). Verification studies on base isolation systems by full-scale building. 1989 *ASME Pressure Vessels and Piping Conference*, Honolulu, Hawaii, PVP-181, pp. 1–8.
- Petersen, N. R. (1980). Design of large scale tuned mass damper. In *Structural Control* (edited by H. H. E. Leipholz). North-Holland, Amsterdam.
- Robinson, W. H. (1982). Lead-rubber hysteretic bearings suitable for protecting structures during earthquakes. *Earthquake Engng Struct. Dynamics* **10**, 593–604.
- Sladek, J. R. and Klingner, R. E. (1983). Effect of tuned-mass damper on seismic response. *J. Struct. Engng ASCE* **109**(8), 2004–2009.
- Tsai, H.-C. (1993). Green's function of support-excited structures with tuned-mass dampers derived by a perturbation method. *Earthquake Engng Struct. Dynamics* **22**, 975–990.
- Tsai, H.-C. and Kelly, J. M. (1988). Non-classical damping in dynamic analysis of base-isolated structures with internal equipment. *Earthquake Engng Struct. Dynamics* **16**, 29–43.
- Tsai, H.-C. and Lin, G.-C. (1993). Optimum tuned-mass dampers for minimizing steady-state response of support-excited and damped structures. *Earthquake Engng Struct. Dynamics* **22**, 957–973.
- Villaverde, R. (1985). Reduction in seismic response with heavily-damped vibration absorbers. *Earthquake Engng Struct. Dynamics* **13**, 33–42.
- Yang, J. N., Danielians, A. and Liu, S. C. (1991). Aseismic hybrid control systems for building structures. *J. Engng Mech. ASCE* **117**(4), 836–853.